

# Influence of *Adansonia Digitata* Leaves Dye Extraction Solvent Nature on the Structural and Physical Properties of Biosynthesized ZnO Nanoparticles

A. O. Kane<sup>1</sup>, S. Thior<sup>1</sup>, NM Ndiaye<sup>1</sup>, B.D. Ngom<sup>1,2,\*</sup>, O. Sakho<sup>1</sup>

<sup>1</sup>Laboratoire de Photonique Quantique, Énergie et NanoFabrication, Faculté des Sciences et Techniques, Université Cheikh Anta Diop de Dakar (UCAD) B.P. 5005 Dakar-Fann Dakar, Sénégal

<sup>2</sup>UNESCO-UNISA Africa Chair in Nanosciences-Nanotechnology, College of Graduate Studies, University of South Africa, Muckleneuk ridge, PO Box 392, Pretoria-South Africa

\*Corresponding author: [bdngom@gmail.com](mailto:bdngom@gmail.com)

Received December 03, 2019; Revised January 12, 2020; Accepted January 19, 2020

**Abstract** We report on the synthesis ZnO nanoparticles with *Adansonia digitata* leaves extract using different extraction solvents: ethanol, methanol, acetone and propanol. The influence of the solvent extraction nature was studied using the characterizations techniques: DRX, BET, SEM, TEM, RAMAN. The results showed the nanoparticles obtained with the solvent Methanol are the best with spherical nanoparticles of sizes around 20 nm with fewer defects and good dispersion compared to those obtained with the other solvents.

**Keywords:** nature of extraction solvent, ZnO nanoparticles, biosynthesis, dyes, characterization and physical properties

**Cite This Article:** A. O. Kane, S. Thior, NM Ndiaye, B.D. Ngom, and O. Sakho, "Influence of *Adansonia Digitata* Leaves Dye Extraction Solvent Nature on the Structural and Physical Properties of Biosynthesized ZnO Nanoparticles." *American Journal of Nanomaterials*, vol. 8, no. 2 (2020): 10-17. doi: 10.12691/ajn-8-1-2.

## 1. Introduction

The bio-resources based synthesis of nanoparticles generated considerable interest as an emerging technology to circumvent high cost in physical synthesis methods and reduce the nanoparticles toxicity commonly associated with conventional chemical synthesis method.

The nanoparticles biosynthesis is a one-step nanoparticle synthesis approach using microorganisms and plants extract. This approach is environment friendly, economical, biocompatible, safe (relatively non-toxic) [1]. It allows the large-scale production of ZnO nanoparticles without additional impurities [2]. Nanoparticles synthesized from a biological approach show greater catalytic activity and limit the use of expensive and toxic chemical products. Green synthesis involves the use of plant extracts, bacteria, fungi, algae, ie. These natural and plant-derived strains secrete certain phytochemicals that act as both a reducing agent and a capping or stabilizing agent [3]. The nature of these biological entities influences the structure, shape, size and morphology of synthesized nanoparticles.

With the advent of biosynthesis, an improvement in the properties of ZnO nanoparticles has been noted. Thus, an increased research has been conducted on their anti-bacterial, anti-catalytic, anti-oxidant, anti-cancer activities etc.... leading to applications in medical fields, water treatment ie....

Several plant extracts such as *Eucalyptus globulus* [4], *Phyllanthus niruri* [5] using *Mangifera indica* leaves [6] have been used to synthesize ZnO nanoparticles. However, the major challenge with this synthesis method is the control of the synthesis parameters such as the pH, temperature, extraction solvent, time ie .... Studies are being done to control these parameters. It is in this context we study the effect of the extraction solvent. Indeed, we synthesized ZnO nanoparticles via a plant extract called *Adansonia digitata* using different solvents: ethanol, methanol, acetone and propanol.

## 2. Experimental Details

### 2.1. Preparation of the Dye Extract of *Adansonia Digitata* Leaves

*Adansonia digitata* leaves were harvested and dried under sunny conditions. A fine powder was obtained after grinding the dried leaves. 3 g of this powder was dissolved in 150 ml of every solvent and stirred for 3 hours at room temperature to ensure maximum extraction of the bioactive compounds. The resulting extract was then filtered to remove residual solids.

### 2.2. Biosynthesis of ZnO Nanoparticles

In 100 ml of this filtered extract, 0.3 g of Zn ( $(\text{NO}_3)_2 \cdot 6\text{H}_2\text{O}$  (zinc nitrate hexahydrate) are dissolved this

solution, after stirring with a magnetic stirrer for 3 hours, the obtained solution is placed in an oven at 300°C for 3 hours for evaporation. The brown powder obtained is then subjected to a heat treatment for 3 h in a free air oven at 500°C: white nanopowders are obtained. Thus we obtained four nanopowders with different solvents.

### 2.3 Characterization of ZnO Nanoparticles

X-ray diffraction (XRD) spectra of the as-prepared ZnO powders were collected using a diffractometer (Bruker D8 Advance) with theta/2theta geometry, operating with a copper tube at 50 kV and 30 mA and reflection geometry at 2 $\theta$  values ranging from 10-90° with a step size of 0.01°. Raman spectroscopy measurements were obtained using a T64000 micro-Raman spectrometer (HORIBA Scientific, Jobin Yvon Technology) with a 514 nm laser wavelength and spectral acquisition time of 120 s was used to characterize the as-prepared samples powders. The morphology of the as-prepared powders was studied using a high-resolution Zeiss Ultra Plus 55 field emission scanning electron microscope (FE-SEM) operated at a voltage of 2.0 kV and a JEOL JEM-2100F high resolution transition electron microscope (HRTEM) at 200 kV. The samples were degassed at 180°C for more than 12 h under vacuum conditions. The surface area was calculated by the Brunauer-Emmett-Teller (BET) method from the adsorption branch in the relative pressure range (P/P<sub>0</sub>) of 0.01-1.0.

## 3. Results and Discussions

### 3.1. Structural Analysis

The Figure 1 presents the X-ray diffraction spectra of the different nanopowders samples obtained using the different solvents. These spectra show diffraction peaks appearing at 2 $\theta$  ranging between 31° and 80° for all the different solvents.

The comparison of the different peak positions obtained with the data of files JCPDS n° 036-1451, 19-1485 and 01-072-110 shows that the obtained powder corresponds to ZnO with a Wurtzite hexagonal structure type.

The values of the lattices parameters *a* and *c* (see Table 1) calculated from the experimental data obtained with the various solvents are in agreement with those found in the literature and in the ZnO JCPDS 036-1451 file (space group: P6<sub>3</sub>mc *a* = 3.24982Å, *c* = 5.20661Å).

**Table 1. Lattices parameters and crystallites size as function of nature of the extraction solvent**

Extraction Solvent	<i>a</i> (nm)	<i>c</i> (nm)	Average crystallites sizes (nm)
Acetone	0,323	0,520	26,92
Propanol	0,324	0,519	28,35
Ethanol	0,325	0,520	18,16
Methanol	0,324	0,519	20,04

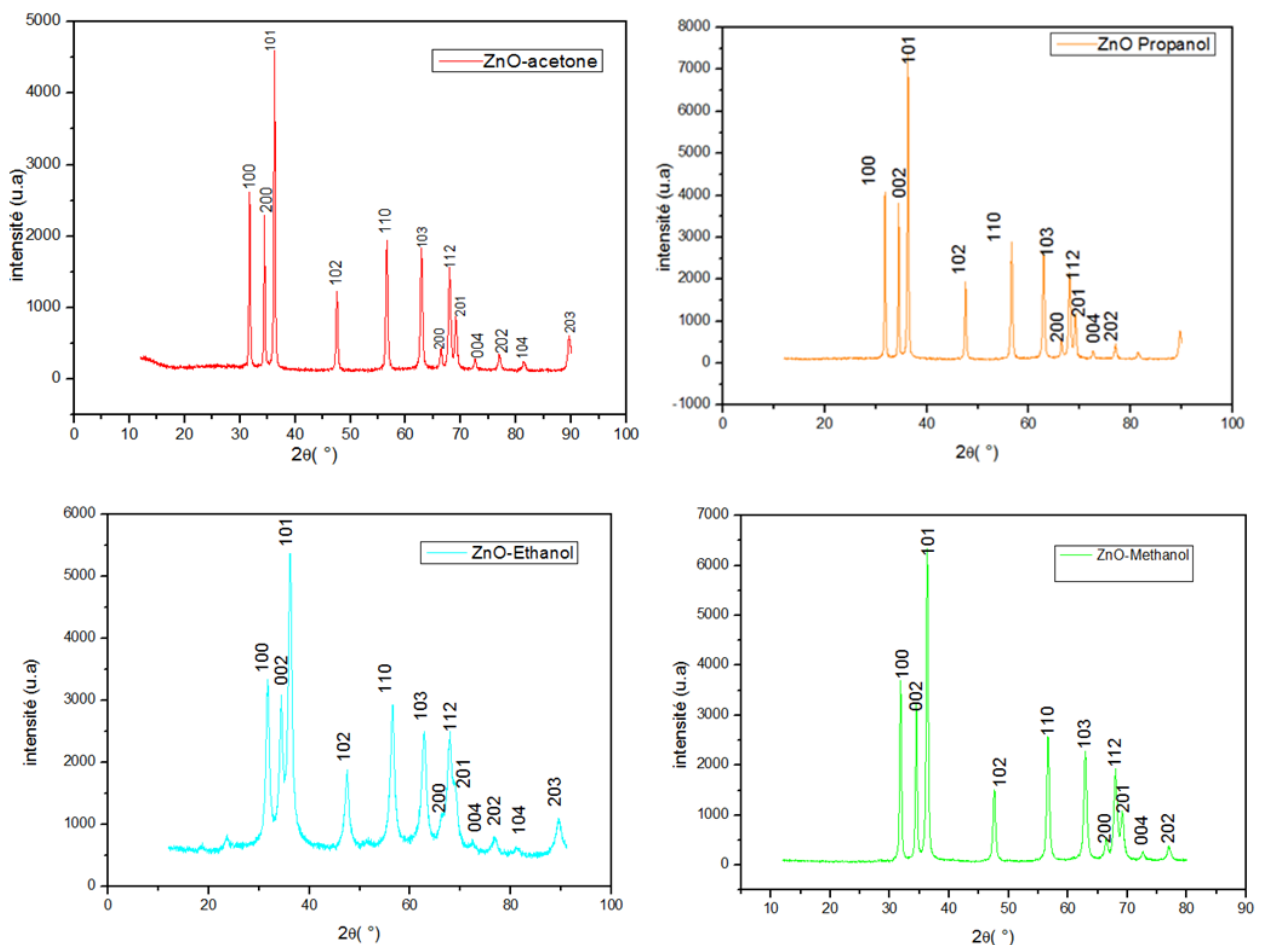


**Figure 1.** DRX spectra of ZnO nanoparticles prepared using different extraction solvent

The nanoparticles obtained with the propanol solvent have larger crystallites sizes than the others, followed by the nanoparticles obtained with the acetone solvent. This size difference would be related, according to Oudhia et al [7], to the boiling points and dielectric constants of the different solvents. These authors explored the effect of *Azadirachta indica* (neem) leaf extract produced in various solvents such as water, ethanol and acetone in the synthesis of ZnO nanoparticles. Indeed, they observed that the leaf extract prepared in water resulted in a lower particle size of ZnO (19 nm) compared to the others solvent (Ethanol at 32 nm and Acetone at 160 nm). The ZnO particles size was correlated with the boiling point and the dielectric constant of the solvent used to prepare the extract. Solvents with higher boiling points and dielectric constants produce larger particles. And at the same time, they also proved that the synthesis process could be controlled by the pH.

Figure 2 (a-d), show the Raman spectra respectively obtained from the prepared nanopowders of ZnO biosynthesized using acetone, propanol, ethanol and methanol as extraction solvents. These Raman scattering spectra of ZnO as function of the various extraction solvents are represented over a frequency range of between 100 and 1400  $\text{cm}^{-1}$ . For the different solvents, except for ethanol In Figure 2 (c), we note the appearance of six active vibration modes of ZnO: E2 (Low), E2 (High) -E2 (Low), A1 (TO), E2 (High), E1 (LO) and 2 A1 (LO) [8] with more or less offset of the position of the peaks depending on the solvents (Table 2). The appearance of the intense peak E2 (High), which is related to oxygen vibrational mode, proves that the nanoparticles obtained with the different solvents have the Wurtzite hexagonal structure and that they crystallized well [8], but with a shift in position and intensity according to the solvents.

**Table 2. Raman modes as function of the extraction solvent**

ZnO-Acetone	ZnO-Propanol	ZnO-Ethanol	ZnO-Methanol	Mode vibrational
101	101	-	101	E2(Low)
335	329	-	331	E2 (high)-E2 (low)
387	382	-	380	A1(TO)
441	439	444	441	E2(High)
583	591	593	585	E1(LO)
1153	1151	-	1152	2A1(LO)

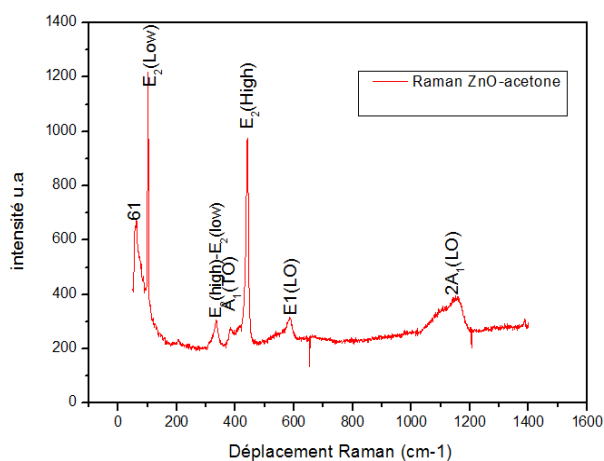


**Figure 2a.** Raman Spectrum of ZnO with Acetone Extraction Solvent

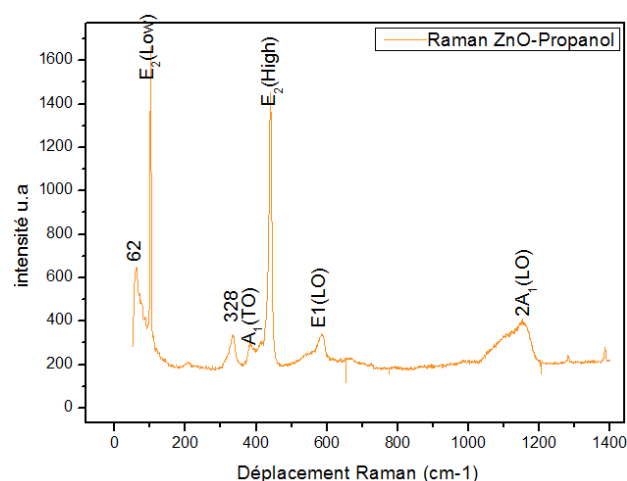


**Figure 2b.** Raman Spectrum of ZnO with propanol Extraction Solvent

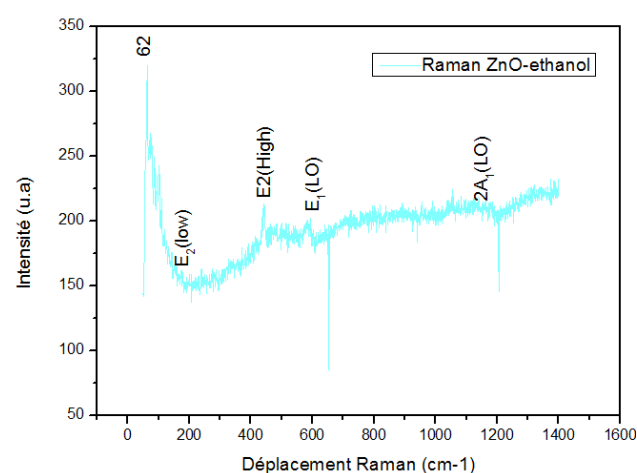


**Figure 2c.** Raman Spectrum of ZnO with ethanol extraction solvent

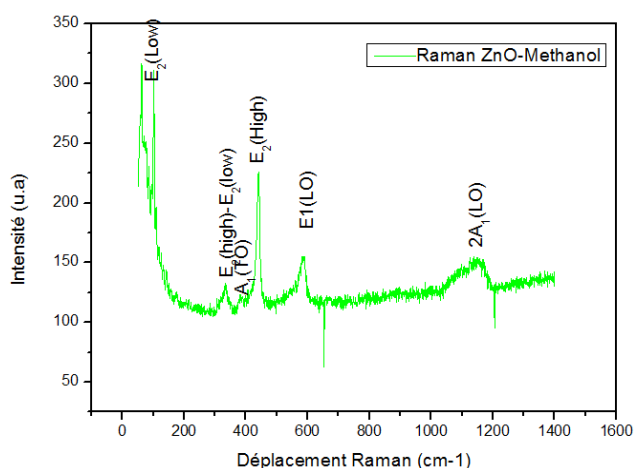


**Figure 2d.** Raman spectrum of ZnO with ethanol extraction solvent

**Table 3. Values of intensities of E2 (High) and crystallite sizes obtained from XRD as function of the solvent**

Extraction Solvent	E <sub>2</sub> (High) intensity	Crystallites sizes (nm)
Acetone	98	26,924
Propanol	1400	28,35
Ethanol	220	18,168
Methanol	250	20,04

This variation in intensity could be related to the difference in size noted with the XRD results. We note that the intensity increases with the size of the nanoparticles (see Table 3), i.e. the crystallinity varies according to solvent as shown in other works.

It is generally accepted that Raman signatures less than  $300\text{ Cm}^{-1}$  are due to vibrations of the Zn interstitial and those above  $300\text{ Cm}^{-1}$  are due to vibrations of the oxygen atoms [9]. E2 (high), 2A1 (LO) and E1 (LO) are very sensitive to lattice disorder in the ZnO [10]. These disorders are generally associated with structural defects such as oxygen vacancies and Zn in interstitial and charge-bearing positions for 2A1 (LO) and E1 (LO) [10]. E2 (H) is sensitive to residual stress in the crystallized ZnO more precisely an increase in the phonon frequency E2 (H) is attributed to the compression stress, whereas a decrease in the phonon frequency E2 (H) is attributed to the constraint traction [11]. In our case we find an increase in frequencies for all solvents compared to that of known crystalline ZnO ( $437\text{ Cm}^{-1}$ ) [8]. So there is the presence of compression stress that varies depending on the solvent. This is reminiscent of the presence of structural defects with all nanoparticles obtained, which is acceptable because in the literature it is well proved that drastic growth conditions such as a high temperature generally induce more defects in the crystals [12]. However, these defects vary depending on the extraction solvent. If we refer to Table 3 we could predict that there would be more defects with the Propanol solvent and fewer defects with the Acetone solvent.

### 3.2. Surface Analysis

The values of the specific surfaces area obtained from BET analysis and the size of the crystallites obtained from XRD analysis are compared in Table 4:

**Table 4.** BET surface specific area and grain size as function of the solvent

Extraction	Specific Surface Area ( $\text{m}^2/\text{g}$ )	Crystallites Sizes (nm)
ZnO-Ethanol	11,8626	18,168
ZnO-Acetone	7,2872	26,924
ZnO-Methanol	7,2131	20,04
ZnO-Propanol	6,1432	28,35

Comparison made between the specific surfaces area with the nanoparticles crystallites sizes obtained from the DRX, showed it is found that there is a net coherence, thus confirming the nanostructuring of the obtained powders. The nanoparticles obtained with ethanol as the extraction solvent are the smaller sizes with a higher surface specific area. Small specific surfaces with acetone and propanol solvents suggest the presence of aggregation of nanoparticles.

The SEM analysis allowed visualizing the surface morphological aspect, namely the uniformity, the porosity, the grain distribution and the approximate sizes of the nanostructured ZnO obtained with the different solvents used. The 2D images obtained by SEM for the various solvents are given in the Figure 3 (a-d).

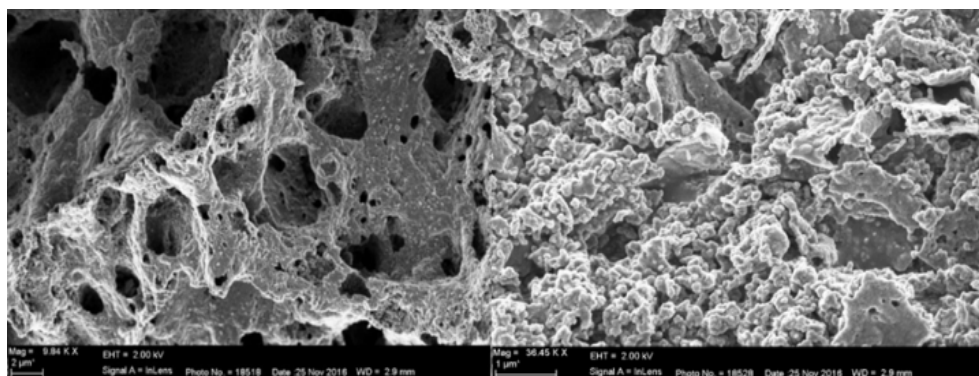


**Figure 3a.** 2DSEM images of ZnO nanopowders obtained from ethanol as solvent

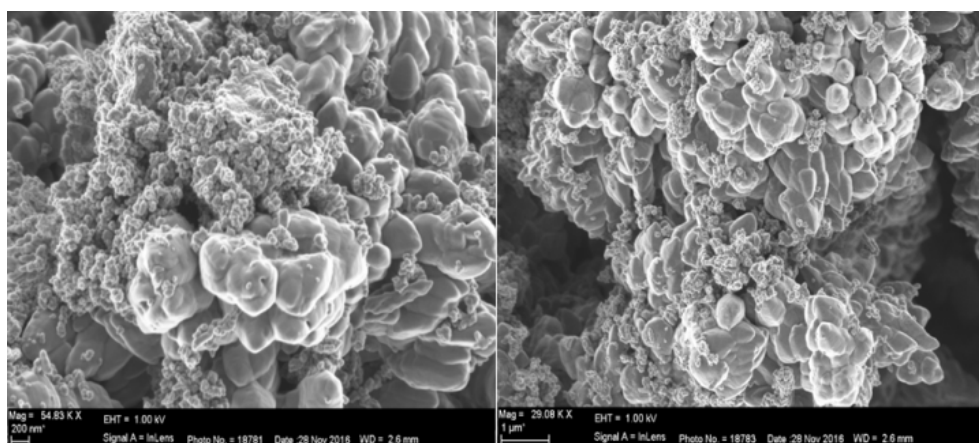


**Figure 3b.** 2DSEM images of ZnO nanopowders obtained from Acetone as solvent

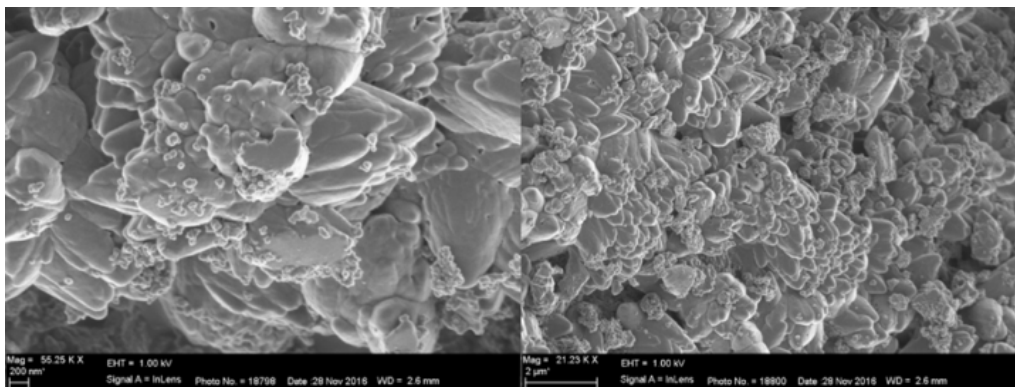


**Figure 3c.** 2DSEM images of ZnO nanopowders obtained from propanol as solvent

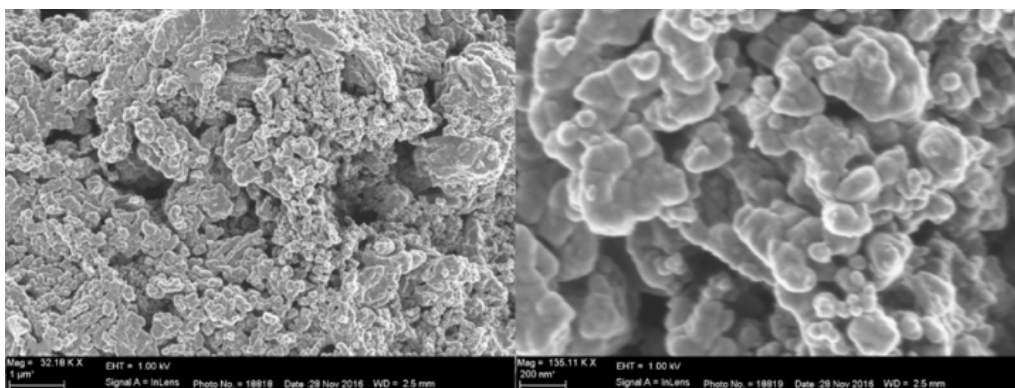


**Figure 3d.** 2DSEM images of ZnO nanopowders obtained from Methanol as solvent

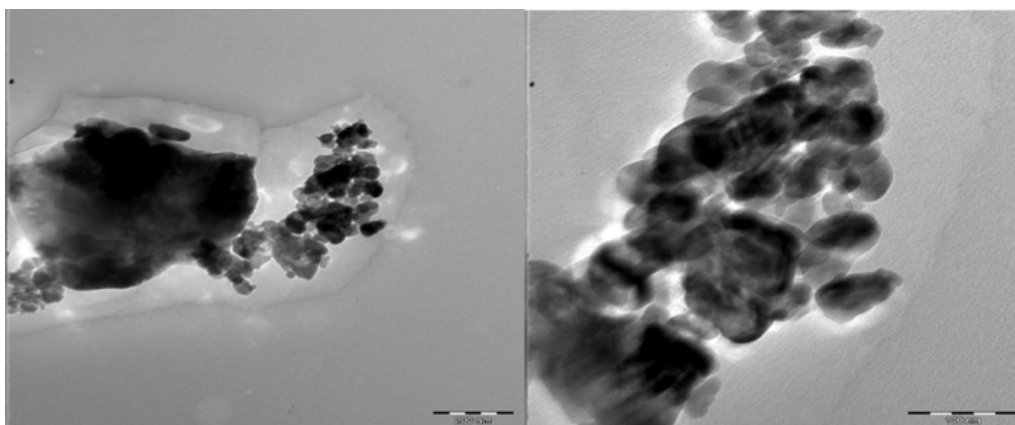


**Figure 4a.** 2DSEM images of ZnO nanopowders obtained from ethanol as solvent

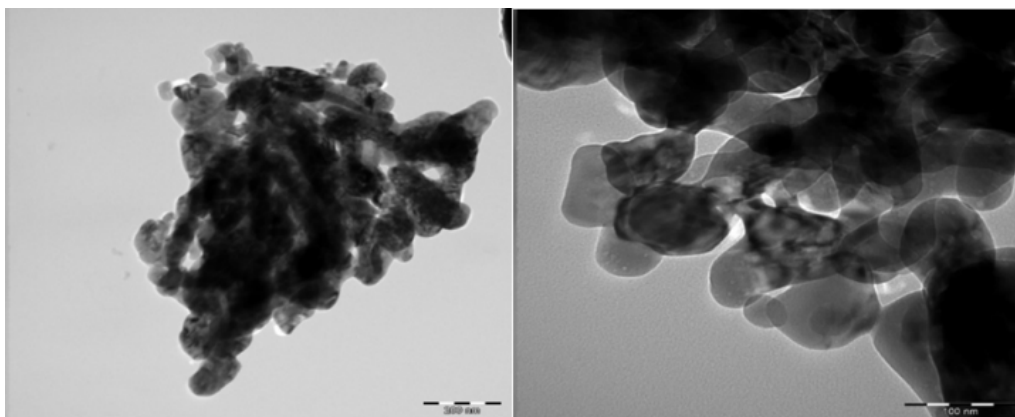


**Figure 4b.** 2DSEM images of ZnO nanopowders obtained from acetone as solvent

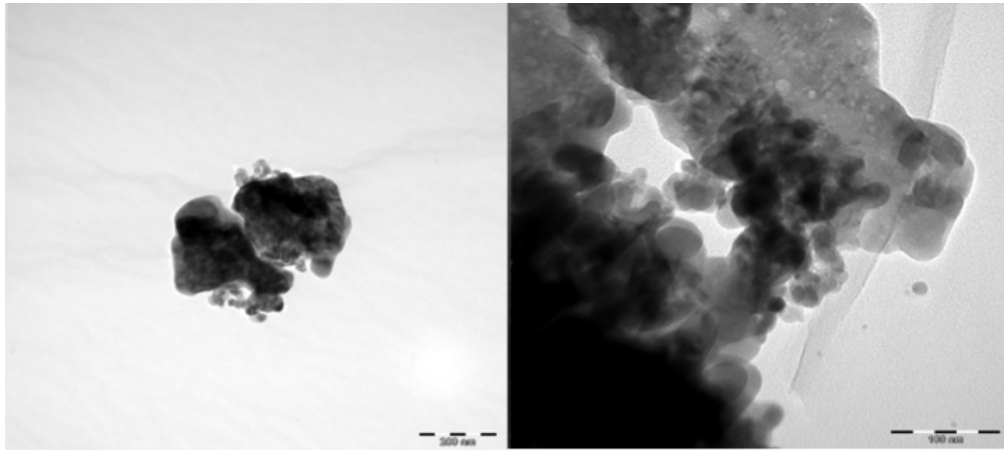


**Figure 4c.** 2DSEM images of ZnO nanopowders obtained from propanol as solvent

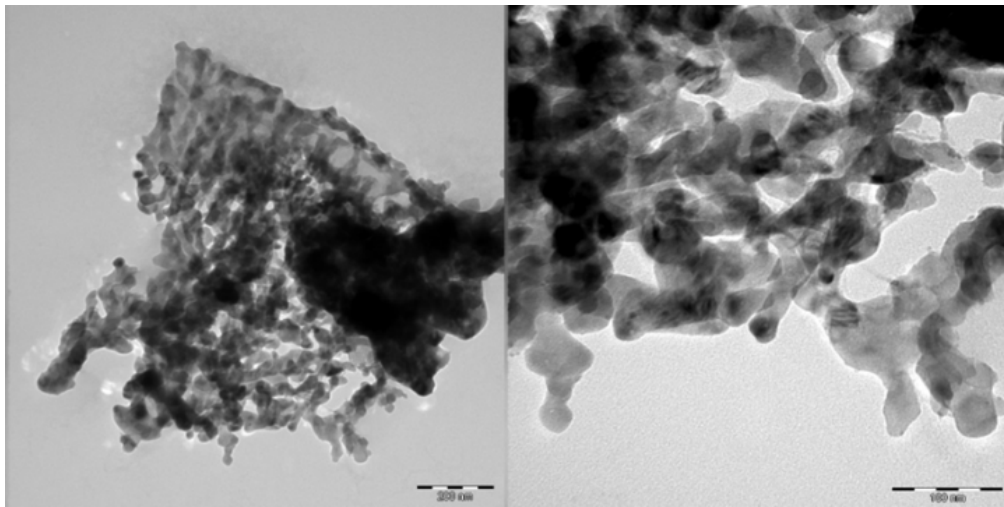


**Figure 4d.** 2DSEM images of ZnO nanopowders obtained from methanol as solvent

The 2D SEM images show, for all the solvents, nanoparticles with a preferentially spherical shape except for those obtained with the solvent Propanol (Figure 3c), which have a conical shape. This spherical shape of the nanoparticles has been obtained by several researchers such as Sangeetha et al. [13] who reported the synthesis of highly stable and spherical ZnO nanoparticles obtained from Aloe vera leaf extracts, as well as Hashemi et al [14].

With the solvent Methanol (Figure 3d) we observe nanoparticles with a more uniform size and a homogeneous nanoparticles distribution with few pores as opposed to those obtained with the ethanol solvent showing very high porosity. With the solvents Acetone and Propanol (Figure 3b and Figure 3c) we observe good crystallized nanoparticles but with disparity in the pores size.

Table 5 gives the grain size calculated from the SEM images using the Image J software.

**Table 5.** Grains sizes calculated from SEM images using Image J software

Solvent	Grains's Sizes from SEM (nm)
ZnO-Acetone	20,66
ZnO-Propanol	21,17
ZnO-Ethanol	13,54
ZnO-Methanol	17,45

To obtain information on the size and shape of ZnO nanoparticles depending on the solvent, Transmission Electron Microscopy (TEM) measurements were also used. The 2D TEM images are presented in the following figures:

The 2D TEM photographs confirm the SEM results. They show for all solvents a predominance of nanoparticles of spherical shapes. A heterogeneous distribution of sizes is observed in all samples, with the formation of aggregates for solvents Propanol, Acetone and ethanol and a presence of significant pores except with the particles from the solvent Methanol and the distribution is more homogeneous with the solvent Methanol. This could explain the differences in values observed with grain sizes calculated from TEM (Table 6), SEM and XRD images. The sizes of the grains calculated from the TEM images differ in values with those obtained with the SEM images but correlate with the results of the XRD.

**Table 6.** Grains sizes obtained from TEM images as function of the solvent

Solvent	Grains's size from TEM (nm)
ZnO-Acetone	27,47
ZnO-Propanol	23,06
ZnO-Ethanol	20,04
ZnO-Methanol	16,15

### 3.3. Discussions

The nanoparticles characterization showed that, during biosynthesis, the extraction solvent choice is decisive because the study proved that the shape, size and nanoparticles dispersion depend on the extraction solvent used. In the literature, this variation in the nanoparticles shape is seen as a benefit because they lead to more diversified applications [15]. Naresh Kumar et al [16] investigated the use of Amorphophallus konjac tuber extract for the synthesis of rice-shaped ZnO nanoparticles for the application of dye-sensitized solar cells. However, the most common form is the spherical shape that has been used very effectively in many areas. Their antioxidant properties [17], antibacterial [18] antidiabetic [19], photocatalytic [20] and others ... are proven. These spherical nanoparticles are also applied as fuels, nanofertilizers used for a rapid growth of tree seedlings in nurseries [21].

The size is one of the key properties of nanoparticles and different ZnO nanoparticles sizes have been synthesized. The lower scale of this size range is based on the measurement of the sieving coefficient for the glomerular capillary wall, since the threshold of first pass elimination by the kidneys is estimated at 10 nm in diameter. The upper scale of the size range is based on the results of various studies showing that, up to 100 nm, the nanoparticles have a better efficiency. Some research shows that nanoparticles less than 10 nm in diameter accumulate more efficiently and penetrate deeper into tumors than their larger counterparts [22].

These nanoparticles homogeneity is also highly sought after because a stable nanoparticles dispersion is useful in fields such as photocatalysis, diodes, piezoelectric devices, fluorescent tubes, lasers and photonics and above all in the medical field where it is essential to control the doses to be administered.

So according to the literature, the ideal sought is spherical nanoparticles of small sizes and very well monodispersed. From our results could conclude that the best solvent in the four is the methanol solvent with a grain size around 20 nm and a more homogeneous nanoparticles sizes distribution. However, in an earlier study, we (Kane et al, 2018) [23] synthesized nanoparticles with the solvent water closer to the ideal because with water as a solvent we obtained spherical nanocrystallines of sizes revolving around 20 nm such as those found by Velmurugan et al [24], with very minimal defects in their structure with a better dispersion than those of nanoparticles with ethanol solvent, so water always remains the best solvent.

### 4. Conclusion

Biosynthesis of zinc oxide nanoparticles which involves zinc nitrate as a precursor, baobab leaves as a natural product and using different extraction solvents: methanol, propanol, ethanol and acetone were studied. The structural properties, crystallites size and surface morphology and properties of the nanoparticles obtained with each extraction solvent were determined using the following characterization methods: DRX, SEM, TEM, BET and

RAMAN and comparative study were made between the results of nanoparticles derived from each solvent.

The results of the characterization showed, for all the solvents, that the particles obtained are crystalline and are in nanometer size with a range of sizes lower than 100 nm for all the solvents. However, the size, shape and dispersion varied with the solvents.

After our comparison we deduced that the nanoparticles synthesized with methanol as extraction solvent is the best because in addition to their spherical shape, they have fewer defects and a better distribution and monodispersivity than other nanoparticles from other extraction solvents. So the best extraction solvent after water is Methanol.

### Acknowledgments

This work was supported by the TWAS-UNESCO Associate Scheme through the University of South Africa (UNISA) as a host institution. The TWAS-UNESCO Associate holder Prof BD Ngom is very thankful to the TWAS-UNESCO as well as the host institution. We are also thankful to iThemba LABS-National Research Foundation of South Africa and the University of Pretoria for the use of their facilities.

### References

- [1] I. Fatimah, R. Y. Pradita, and A. Nurfalinda, "Plant Extract Mediated of ZnO Nanoparticles by Using Ethanol Extract of Mimosa Pudica Leaves and Coffee Powder," *Procedia Eng.*, vol. 148, pp. 43-48, 2016.
- [2] R. Yuvakkumar, J. Suresh, A. J. Nathanael, M. Sundrarajan, and S. I. Hong, "Novel green synthetic strategy to prepare ZnO nanocrystals using rambutan (*Nephelium lappaceum* L.) peel extract and its antibacterial applications," *Mater. Sci. Eng. C*, vol. 41, pp. 17-27, 2014.
- [3] Y. Zong, Z. Li, X. Wang, J. Ma, and Y. Men, "Synthesis and high photocatalytic activity of Eu-doped ZnO nanoparticles," *Ceram. Int.*, vol. 40, no. 7 PART B, pp. 10375-10382, 2014.
- [4] B. Siripireddy and B. K. Mandal, "Facile green synthesis of zinc oxide nanoparticles by Eucalyptus globulus and their photocatalytic and antioxidant activity," *Adv. Powder Technol.*, vol. 28, no. 3, pp. 785-797, 2017.
- [5] M. Anbuvarnan, M. Ramesh, G. Viruthagiri, N. Shanmugam, and N. Kannadasan, "Synthesis, characterization and photocatalytic activity of ZnO nanoparticles prepared by biological method," *Spectrochim. Acta - Part A Mol. Biomol. Spectrosc.*, vol. 143, pp. 304-308, 2015.
- [6] S. Rajeshkumar, S. V. Kumar, A. Ramaiah, H. Agarwal, T. Lakshmi, and S. M. Roopan, "Biosynthesis of zinc oxide nanoparticles using *Mangifera indica* leaves and evaluation of their antioxidant and cytotoxic properties in lung cancer (A549) cells," *Enzyme Microb. Technol.*, vol. 117, pp. 91-95, 2018.
- [7] A. Oudhia, S. Sharma, P. Kulkarni, and R. Kumar, "Blue emitting ZnO nanostructures grown through cellulose bio-templates," *Luminescence*, vol. 31, no. 4, pp. 978-985, 2016.
- [8] A. F. Jaramillo *et al.*, "Estimation of the surface interaction mechanism of ZnO nanoparticles modified with organosilane groups by Raman Spectroscopy," *Ceram. Int.*, vol. 43, no. 15, pp. 11838-11847, 2017.
- [9] S. Khachadorian *et al.*, "Effects of annealing on optical and structural properties of zinc oxide nanocrystals," *Phys. Status Solidi Basic Res.*, vol. 252, no. 11, pp. 2620-2625, 2015.
- [10] M. Gomi, N. Oohira, K. Ozaki, and M. Koyano, "Photoluminescent and structural properties of precipitated ZnO fine particles," *Japanese J. Appl. Physics, Part 1 Regul. Pap. Short Notes Rev. Pap.*, vol. 42, no. 2 A, pp. 481-485, 2003.

- [11] Y. Huang, M. Liu, Z. Li, Y. Zeng, and S. Liu, "Raman spectroscopy study of ZnO-based ceramic films fabricated by novel sol-gel process," *Mater. Sci. Eng. B Solid-State Mater. Adv. Technol.*, vol. 97, no. 2, pp. 111-116, 2003.
- [12] B. Cao, W. Cai, Y. Li, F. Sun, and L. Zhang, "Ultraviolet-light-emitting ZnO nanosheets prepared by a chemical bath deposition method," *Nanotechnology*, vol. 16, no. 9, pp. 1734-1738, 2005.
- [13] G. Sangeetha, S. Rajeshwari, and R. Venckatesh, "Green synthesis of zinc oxide nanoparticles by aloe barbadensis miller leaf extract: Structure and optical properties," *Mater. Res. Bull.*, vol. 46, no. 12, pp. 2560-2566, 2011.
- [14] S. Hashemi, Z. Asrar, S. Pourseyedi, and N. Nadernejad, "Plant-mediated synthesis of zinc oxide nano-particles and their effect on growth, lipid peroxidation and hydrogen peroxide contents in soybean," *Indian J. Plant Physiol.*, vol. 21, no. 3, pp. 312-317, 2016.
- [15] Z. L. Wang, "Nanostructures of zinc oxide," *Mater. Today*, vol. 7, no. 6, pp. 26-33, 2004.
- [16] P. N. Kumar, K. Sakthivel, and V. Balasubramanian, "Microwave assisted biosynthesis of rice shaped ZnO nanoparticles using *Amorphophallus konjac* tuber extract and its application in dye sensitized solar cells," *Mater. Sci. Pol.*, vol. 35, no. 1, pp. 111-119, 2017.
- [17] B. N. Singh, A. K. S. Rawat, W. Khan, A. H. Naqvi, and B. R. Singh, "Biosynthesis of stable antioxidant ZnO nanoparticles by *Pseudomonas aeruginosa* Rhamnolipids," *PLoS One*, vol. 9, no. 9, 2014.
- [18] E. J. Ibrahim, K. M. Thalij, M. K. Saleh, and A. S. Badawy, "Biosynthesis of zinc oxide nanoparticles and assay of antibacterial activity," *Am. J. Biochem. Biotechnol.*, vol. 13, no. 2, pp. 63-69, 2017.
- [19] N. Bala *et al.*, "Green synthesis of zinc oxide nanoparticles using *Hibiscus subdariffa* leaf extract: Effect of temperature on synthesis, anti-bacterial activity and anti-diabetic activity," *RSC Adv.*, vol. 5, no. 7, pp. 4993-5003, 2015.
- [20] J. Fowsiya, G. Madhumitha, N. A. Al-Dhabi, and M. V. Arasu, "Photocatalytic degradation of Congo red using *Carissa edulis* extract capped zinc oxide nanoparticles," *J. Photochem. Photobiol. B Biol.*, vol. 162, pp. 395-401, 2016.
- [21] S. K. Chaudhuri and L. Malodia, "Biosynthesis of zinc oxide nanoparticles using leaf extract of *Calotropis gigantea*: characterization and its evaluation on tree seedling growth in nursery stage," *Appl. Nanosci.*, vol. 7, no. 8, pp. 501-512, 2017.
- [22] T. Vivo, "Size-Dependent Localization and Penetration of Ultrasmall Gold Nanoparticles in Cancer Cells, Multicellular," *ACS Nano*, vol. 6, no. 5, pp. 4483-4493, 2012.
- [23] A. O. Kane *et al.*, "Biosynthesis of ZnO Nanoparticles by *Adansonia Digitata* Leaves Dye Extract: Structural and Physical Properties," *MRS Adv.*, vol. 3, no. 42-43, pp. 2487-2497, 2018.
- [24] P. Velmurugan *et al.*, "Eco-friendly approach towards green synthesis of zinc oxide nanocrystals and its potential applications," *Artif. Cells, Nanomedicine Biotechnol.*, vol. 44, no. 6, pp. 1537-1543, 2016.



© The Author(s) 2020. This article is an open access article distributed under the terms and conditions of the Creative Commons Attribution (CC BY) license (<http://creativecommons.org/licenses/by/4.0/>).